Tellus (1995), 47A, 797–814
Printed in Belgium – all rights reserved

TELLUS
ISSN 0280–6495

Numerical simulations of the synoptic conditions and development of Arctic outbreak polar lows

By SIGBJØRN GRØNÅS* and NILS GUNNAR KVAMSTØ, *Geophysical Institute, University of Bergen, Allégaten 70, 5007 Bergen, Norway*

(Manuscript received 5 September 1994; in final form 15 December 1994)

ABSTRACT

Four cases satisfying the necessary conditions for development of Arctic outbreak polar lows have been investigated from numerical simulations. Characteristic synoptic conditions are a mature extratropical cyclone situated over Scandinavia and a northerly, baroclinic flow in the Norwegian Sea. This flow has a convective planetary boundary layer (PBL) caused by heat fluxes from the warm ocean in cold Arctic air masses coming from the sea ice areas to the north and west. The height of the PBL may reach 700 hPa and even more. The synoptic situation is also characterized by a dry intrusion of stratospheric air west of the cyclones. When the tropopause is defined by the surface of potential vorticity (PV) equal 2 PVU (1 PVU = $10^{-6}\,m^2\,s^{-1}\,K\,kg^{-1}$), the intrusion lowers the tropopause typically down to levels between 450 and 750 hPa, bringing large positive anomalies of PV to levels normally in mid-troposphere. These synoptic conditions are ideal for cyclogenesis from mutual interaction of positive upper air and boundary layer PV anomalies. The Rossby height is high, which means that small-scale polar lows may form. It is found that simply the height between the tropopause and the top of the convective PBL is a good indicator of the risk of polar low formation. This height was found to be 2500 m or more in two of the cases when no polar lows were observed. When polar lows developed in the other two cases, heights of 1000 m or less were measured (in numerical simulations). The simulated development of these two polar lows has been investigated. The polar low cyclogenesis was found to be caused by the baroclinic instability in agreement with the conceptual model of Montgomery and Farrel. Diabatic intensification is important and seems to be necessary to seclude the warm core disturbance which is characteristic of Arctic outbreak polar lows. The seclusion process implies that warm air is being surrounded by cold air.

1. Introduction

Polar lows are cyclones on the sub-synoptic scale formed over high-latitude oceans polewards of the polar front. Polar lows span scales from less than 100 km to more than 1000 km in diameter, and show a wide range of intensities, from strong breezes to hurricane force winds. They may form within a few hours and last from hours to several days. Some polar lows show a resemblance to mature tropical cyclones, exhibiting strong surface winds and an "eye" surrounded by deep cumulonimbi clouds.

A theoretical quantitative explanation of polar lows has been sought in baroclinic instability theory (Harrold and Browning, 1969; Mansfield, 1974; Reed, 1979; Duncan, 1977, 1978; Reed and Duncan, 1987), conditional instability of second kind (CISK) (Rasmussen, 1977, 1979; Økland, 1977, 1987, 1989; van Delden 1989a, b; Bratseth, 1985), and air-sea interaction instability (Emanuel, 1986; Emanuel and Rotunno, 1989).

Normal mode studies on baroclinic instability give e-folding times of one day or more. However, observations indicate more rapid development, with mature polar lows evolving within less than a day, sometimes within a few hours. Other theoretical work on baroclinic growth focusses on the effect of reduced low-level static stability,

* Corresponding author.

either due to direct latent heating (Gall, 1976) or variable static stability in a dry model (Staley and Gall, 1977; Blumen, 1979; Wiin-Nielsen, 1989). A decreased static stability increases the normal mode growth and widens the range of unstable wave numbers to smaller scales. However, recent work places upper bounds on the growth. Even in the limit of conditional neutral stratification, the growth rates are no more than twice those of the corresponding dry system (Emanuel et al., 1987; Joly and Thorpe, 1989).

In CISK theory polar lows are regarded to form from disturbances that utilize convective available potential energy (CAPE) through a mutual feedback between cumulus clouds and large-scale moisture convergence. It has been shown by Ooyama (1982) and van Delden (1989a, b) that CISK is only active after a finite amplitude vortex has attained sufficient strength and organization. Thus CISK may describe only a portion of the intensification. The air-sea interaction instability also needs a well-developed vortex to initiate the development. The growth rates obtained seems to be too slow to explain observed polar lows.

Observational case studies and numerical simulations of polar lows suggest that they are generally initiated by mobile upper-level disturbances (for references see review articles by Businger and Reed, 1989; Grønås, 1992). Further, these studies indicate that polar low formation involves combined effects of upper air forcing, strong surface baroclinicity, deep moist convection, and strong fluxes of latent and sensible heat from the ocean. A two stage development has often been indicated, the first as a baroclinic development connected to a disturbance aloft, and the second as an intensification on a smaller scale caused by diabatic heating.

The strong link of polar lows to finite-amplitude upper-level disturbances suggests that the formation of polar lows should be studied as an initial value problem as done by Farrell (1982, 1984) for extratropical cyclones. The potential vorticity (PV) perspective, reviewed and extended by Hoskins et al. (1985), offers a concept of diagnosis. Montgomery and Farrell (1992) used a nonlinear geostrophic momentum model, which incorporated moist processes and included strong baroclinic dynamics. Based on results from integrations from idealized initial conditions, believed to be typical for polar lows, they proposed a conceptual model in two stages. In the first stage a mobile upper trough initiates a rapid low-level spin-up due to the enhanced omega response in a conditionally neutral atmosphere. A second stage follows through diabatic intensification associated with the production of low-level PV by diabatic processes. Diabatic intensification represents a mechanism for maintaining the intensity of polar lows until they reach land. As a consequence of this model, polar lows are formed in the same way as strong explosive extratropical cyclones, with moist processes playing a more central role in the polar low case.

With definitions of polar lows used in studies of their occurrence in the Norwegian and Barents Sea (Wilhelmsen, 1985; Lystad et al., 1986), polar lows are found in northerly flows. However, such polar lows are not usually observed in westerly flows crossing Scandinavia, although deep convection and troughs in cold air masses are very common. A theory of polar lows must also explain this fact. Økland (1987, 1989) claimed that the clue must lie in the convective boundary layer, where the top comprises the Arctic inversion, being formed in northerly flows as cold air over the ice is advected over the warm sea. Local deeper convection may then be formed underneath upper air disturbances, and CISK may be initiated. Elsewhere, deep convection is inhibited by the strong inversion capping the polar planetary boundary layer (PBL). In westerly flows the Arctic inversion and the strong low-level baroclinicity is normally lacking, and more homogenous regions of deep convection are observed in the cold air masses behind extratropical cyclones.

In the Norwegian and Barents Seas, the northerly flow and the Arctic inversion seem to be necessary conditions for polar lows to develop (Wilhelmsen, 1985, Businger and Reed, 1989). In this paper we discuss four cases which all satisfy these conditions for polar low formation. In two cases no polar low was observed, and in the other two cases polar lows were formed. In addition to the convective boundary layer, the role of the stratospheric, dry intrusion (Browning, 1990), organized behind extratropical cyclones crossing Scandinavia, is investigated. The cases are studied from simulations using the Norwegian operational numerical model. When polar lows are simulated, the developments are studied in terms of PV structures of the upper level forcing and their interaction with low-level temperature anomalies and diabatic processes. Since upper air mobile disturbances seem to play an important part in the formation of polar lows connected to Arctic outbreaks, we propose a modification of the classification of polar lows introduced by Businger and Reed (1989). Maps showing the height of the convective boundary layer and the height of the tropopause are proposed for operational forecasting of the risk of polar lows.

2. Four cases with synoptic conditions for Arctic outbreak polar lows

Four cases in the Norwegian Sea from late winter and spring, which all fulfil normal synoptic conditions for the formation of polar lows (Wilhelmsen, 1985; Lystad et al., 1986), have been chosen. Mature extratropical cyclones are situated over the Scandinavian region. They steer northerly surface flows over the Norwegian Sea. Cold air masses are being advected from the sea ice in the north (for positions, see Fig. 1) and a convective PBL has been formed over the sea by strong fluxes of sensible and latent heat. The well mixed PBL is separated from the upper cold, stable polar air masses by a strong Arctic inversion. The capping inversion descends to the sea surface at the leading edge of the cold air outbreak forming what is here referred to as the Arctic front. Following the classification of polar lows proposed by Businger

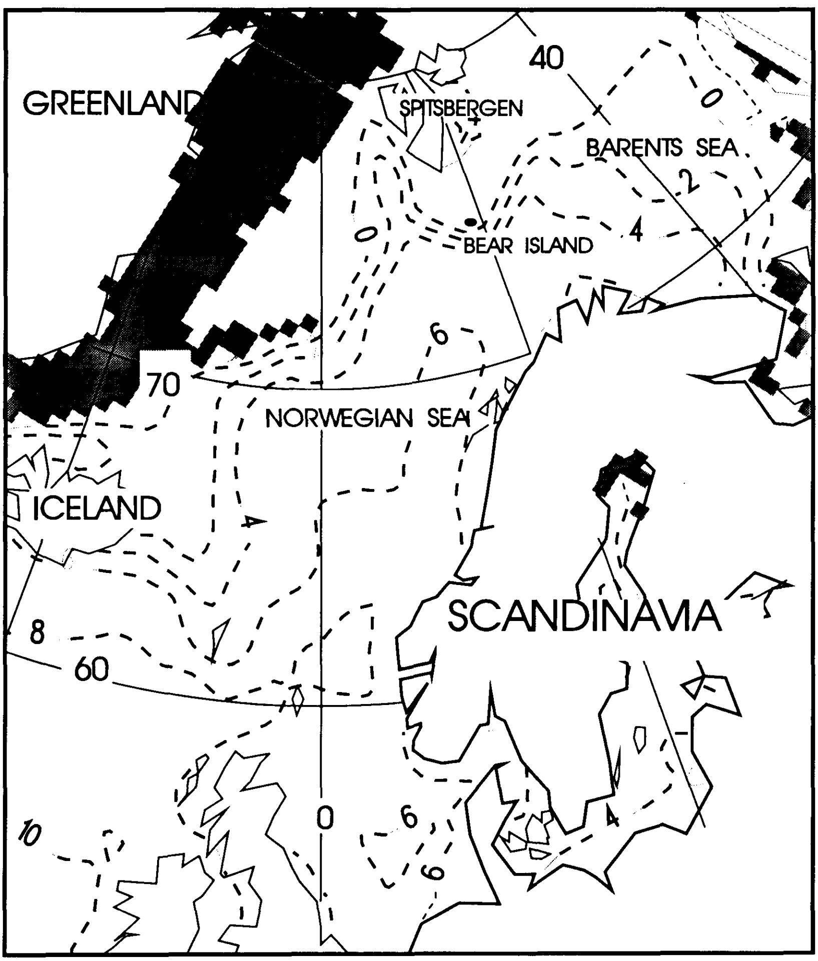

Fig. 1. The geographical area. Dashed lines: SST middle March 1992 (contour step 2°C). Shaded area: Sea ice.

and Reed (1989), these conditions should be favourable for what they called Arctic front polar lows. In their classification this type is associated with ice boundaries and characterized by shallow baroclinicity and strong surface fluxes. The expression "Arctic front polar lows" will not be used in this paper since the disturbances not seem to be directly associated with the leading edge of the Arctic inversion. Instead "Arctic outbreak polar lows" will be used.

In two of the situations no polar low development is observed, and in the other two cases polar low formations occur. The difference in satellite pictures (Figs. 2a, b) despite similarities in synoptic conditions from the two cases is striking. In Fig. 2a no sign of polar lows is seen. The convective PBL is clearly shown by regular streets of cumulus clouds with growing heights southwards. In Fig. 2b several mesoscale vortices representing polar lows are seen in the northerly flow. Numerical simulations of the cases have been made and studied to find characteristic differences in the synoptic conditions, differences that might explain the presence or absence of polar lows. The simulated

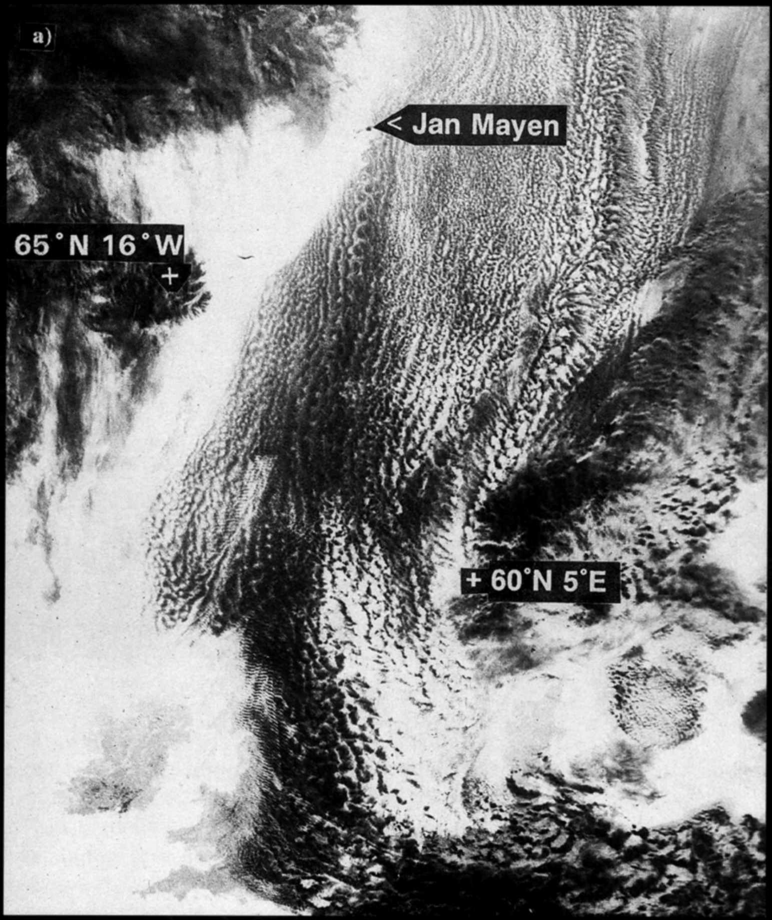

Fig. 2. (a) Satellite (NOAA-11) image over the North Sea and the Norwegian Sea 16 April 1991 about 1300 UTC. The composite picture is based on AVHRR channel 2 (visual) data. (Satellite receiving Station is Dundee University, United Kingdom.) (b) Satellite (NOAA-11) image over the North Sea and the Norwegian Sea 15 April 1992 about 0430 UTC. The composite picture is based on AVHRR channel 4 (infrared) data. (Satellite receiving Station is Dundee University, UK.)

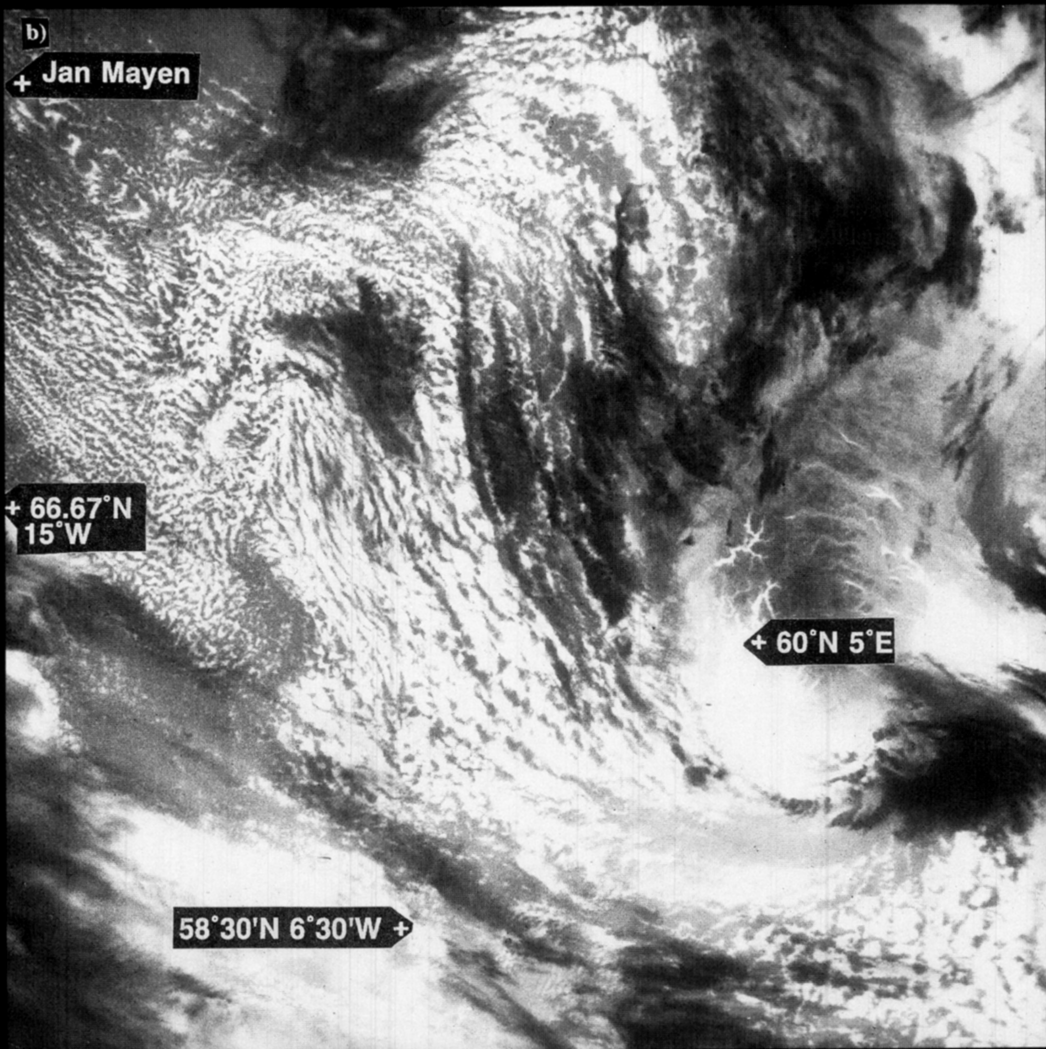

Fig. 2. (cont'd).

developments in one of the cases (*Case D*) are described in Section 5.

In this way the present study is a model-based diagnostic study. It is our belief that an acceptable numerical simulation represents a reasonable representation of the true development. The four simulations have the following initial dates: 00 UTC 3 April 1990, 00 UTC 16 April 1991, 12 UTC 26 February 1987 and 12 UTC 13 March 1992. These cases will be referred to as Case A, B, C and D respectively. They are simulated with the Norwegian limited area model (Grønås and Hellevik, 1982; Nordeng, 1986; Grønås and Midtbø, 1987), with the extension to the hydrological cycle according to Sundqvist et al. (1989). The main attraction with this scheme is that it carries cloud water as a prognostic variable. The horizontal mesh has been 50 km at 60° N on a stereographic map and the integration domain covered 121×97 grid-points. Vertically there have been 18 sigma levels between 100 hPa and the surface. Different integration areas have been used.

Analyses and lateral boundary conditions have been taken from ECMWF analyses interpolated to pressure surfaces. Surface parameters including the sea surface temperature (SST) have been taken from the Norwegian operational model. In this routine detailed SST maps are analyzed subjectively from available surface observations and satellite information. The simulations have been compared with satellite images and surface weather maps from the Western Norway Weather Office.

The simulation results, represented by prognostic and diagnostic variables, have been interpolated to surfaces of potential temperature (θ) and PV respectively. In this way we have been able to display both PV in θ-surfaces and θ in PV surfaces. Instead of using θ we prefer to present pressure (p) of the PV surfaces in our figures. Some difficulties were met in displaying variables in PV surfaces, since they are far from horizonal in the troposphere, and even closed surfaces are present. Horizontal maps of the height of the boundary layer were found valuable and were made from vertical interpolation of the vertical stability.

3. Two cases without polar low development

3.1. *Case A*

In the beginning of this simulation a mature, decaying extratropical cyclone is centred over southern Scandinavia (Fig. 3a). Stratospheric air has descended west of the low. This dry intrusion (Browning, 1990) has left surpluses of high PV at tropospheric levels. To depict the dry intrusion, the height of the 2 PVU surface was found suitable. This height after 6 h integration is shown in Fig. 3a. We let this surface also represent the tropopause, which has descended down to almost 500 hPa. Cold air from the ice has been advected southwards, a convective PBL has been formed and areas with large low-level baroclinicity are found. This is seen from Fig. 3b, which shows the height of the convective PBL and the potential temperature (θ) at 925 hPa. The low-level northerly baroclinic flow is situated beneath the upper reservoir of PV and surface heat fluxes are considerable. In this way, favourable conditions for polar lows are present. The conditions for polar lows to develop did not change much later in the simulation, and no polar low was indicated by the simulation, the observations or the satellite images.

A potential region for initiating a development is found below the upper PV anomaly situated at 60° N 10° W, where the stratospheric fold nearly reaches the 500 hPa level. The height of the convective PBL beneath the PV anomaly is close to 2000 m. The surface temperature anomaly, with which the PV anomaly can interact, is rather weak. Mutual interaction is controlled by the Rossby height $H \sim f_e L/N$, where L is a horizontal scale of the disturbance being formed, N is the Brunt-Väisällä frequency and f_e is an effective local Coriolis parameter given by the strength of the disturbance (Hoskins et al., 1985). In our cases the Rossby height seems to be mainly controlled by the vertical stability (N). Instead of estimating the Rossby height, we simply find that the height between the tropopause and the top of the PBL, together with the strength of the PV anomalies, are suitable parameters for evaluating the risk of polar low development. At the present position this height seems to be too large (more than 3000 m) to initiate any mutual interaction to form a polar low.

Another critical area is connected to the second PV anomaly further north, at 73° N, 2° E. Beneath this anomaly the convective boundary layer is well developed, reaching more than 2500 m, and the surface baroclinicity is large. However, the closest upper PV anomaly just reaches the 450 hPa level, so also here the height between this anomaly and the inversion seems to be too large to create a polar low (more than 3000 m).

3.2. *Case B*

A decaying extratropical cyclone has in the beginning its surface pressure centre over northeastern Scandinavia (Figs. 3c, d). As in the previous case a dry intrusion has taken place with an upper tropospheric PV reservoir. Below is situated a low-level baroclinic flow in a convective PBL. The deepest PV anomaly is situated off the coast of Southern Norway with an extension over land. This anomaly nearly reaches down to 550 hPa. Underneath is found a convective boundary layer reaching more than 2000 m. The vertical distance in this case is less than in the former case (between 2500 and 3000 m). However, the surface temperature anomaly is rather weak. Besides, the position

Fig. 3. (a) Simulation (6 h) of SLP (thin solid lines, contour step 5 hPa) and the pressure of the 2 PVU surface (thick solid lines, contour step 50 hPa), valid at 06 UTC 3 April 1990 (Case A). 1 PVU = 10^{-6} m^2 s^{-1} K kg^{-1}. (b) Simulation (6 h) of θ at 925 hPa (thin solid lines, contour step 3 K) and the height of the planetary boundary layer (thick solid lines contour step 500 m). The fields are valid at 06 UTC 3 April 1990 (Case A). (c) Same as (a), but valid at 06 UTC 16 April 1991 (Case B). (d) Same as (b), but valid at 06 UTC 16 April 1991 (Case B).

of the anomalies close to the coast, with an on-shore wind component, is an unfavourable position for a polar low development.

As in the first case the convective boundary layer is well developed south of Spitsbergen with strong surface temperature anomalies being formed over the tongue of warm sea surface present in this area. Many polar lows form on such anomalies from this area, Grønås et al. (1987). However, in this case no PV anomaly aloft is found and no polar low was formed.

During the simulation the synoptic conditions did not change to give more favourable conditions for polar lows.

4. Two cases with polar low development

4.1. *Case C*

A polar low formation took place in the Bear Island region 26 and 27 February 1987. This development has been studied and described in detail by Nordeng and Rasmussen (1992). The precursor of this development was an extratropical cyclone of rather small scale in the Norwegian Sea, crossing eastward towards the Barents Sea during the 25 February. Around 12 UTC 26 February the cyclone occluded, had a central pressure of about 995 hPa and was situated over the Barents Sea near 74° N 30° E (Fig. 4a). In the rear of the low a northwesterly flow advected cold air from the ice out over the ocean. In addition, a dry stratospheric intrusion took place, which resulted in high values of PV at low tropospheric levels. In the 6-h simulation, we observe that the tropopause has been folded down to 650 hPa (Fig. 4a). The maximum

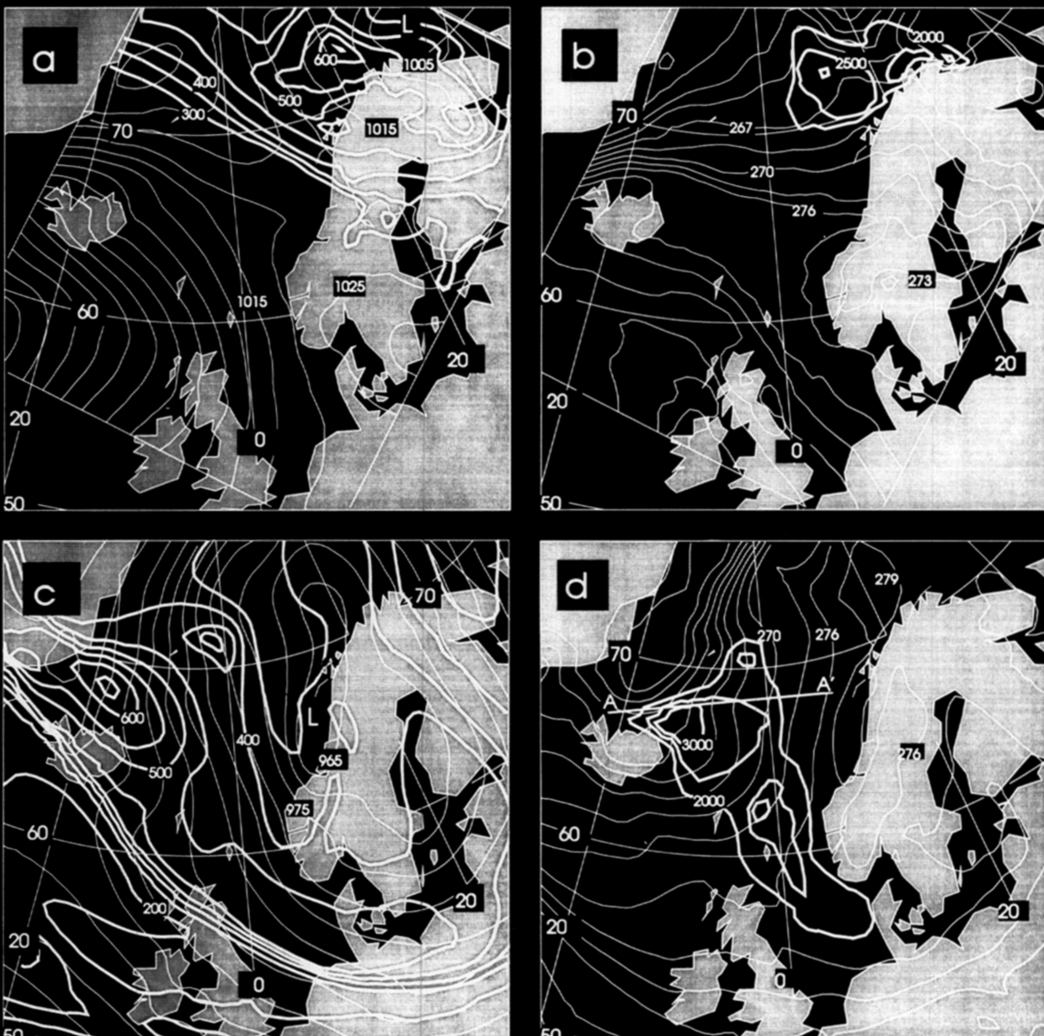

Fig. 4. (a) Same as Fig. 3a, but valid at 18 UTC 26 February 1987 (Case C). (b) Same as Fig. 3b, but valid at 18 UTC 26 February 1987 (Case C). (c) Same as Fig. 3a, but valid at 18 UTC 13 March 1992 (Case D). (d) Same as Fig. 3b, but valid at 18 UTC 13 March 1992 (Case D).

height of the PBL reaches 3000 m and is situated right beneath the upper PV anomaly (Fig. 4b). The height between the two surfaces is less than 1000 m and close contact between the surface temperature anomaly and the upper level PV anomaly is provided. Mutual interaction triggers a polar low development. Our simulations are very similar to the simulations by Nordeng and Rasmussen (1992), and for a detailed description of the development, we refer to their paper.

4.2. Case D

In the beginning a synoptic-scale low is situated over Scandinavia and a northerly surface flow in the Norwegian Sea (Fig. 4c). Cold air from the ice is being advected over the ocean and strong horizontal temperature gradients are present in a convective PBL (Fig. 4d). As is often the case, the flow direction at the surface is from northwest, but the low-level thermal wind is in the opposite direction. This structure is referred to as one of reversed shear. The dry intrusion of stratospheric PV behind the synoptic-scale low is strong. North of Iceland a large anomaly is present with a diameter of 900 km at 550 hPa. The tropopause has been folded down to 650 hPa (Fig. 4c). Beneath this PV anomaly the top of the PBL is higher than 3000 m, which means a vertical distance less than 1000 m between the two surfaces. Indeed, the conditions must be favourable for a polar low to form.

We notice the small horizontal distance (200 km) between the position of maximum boundary layer height and the sea ice border off the coast of Greenland. According to studies of the convective PBL by Økland (1983), this height is far too large to be formed by heating from the ocean only. Below the upper PV anomaly vertical stability is generally low (Hoskins et al., 1985) and the local maximum of the height of the convective layer is formed by the PV anomaly aloft. The PV anomaly is moving towards the southeast, and the boundary layer is being raised by the vertical velocities caused by the so-called "vacuum cleaner effect" (Hoskins et al., 1985) of the approaching PV anomaly.

A second polar low was developed from large surface temperature anomalies formed over the open, warm ocean west of Spitsbergen in interaction with the same upper PV anomaly. It formed when the surface anomaly was advected southwards and came in contact with the PV reservoir northeast of Iceland. We notice the similarities in the surface conditions with case B when no upper PV anomaly was available and no polar low was formed. Theoretically, it is shown by Montgomery and Farrel (1992) that polar lows may form without any upper level disturbance. However, to our knowledge no such polar low case has been reported.

Since the lower-level disturbance is related to the geographical position west of Spitsbergen, the two lows seem to develop independently of each other, and not in a train as observed by Reed and Duncan (1987).

5. Simulations of polar lows in Case D

The first sign of the development of a polar low east of Iceland is found after 6 hours of simulation (Figs. 4c, d). At the surface a weak, warm trough has been formed. When this perturbation is withdrawn from the large-scale, baroclinic flow, it shows a shape of an ellipse with the longest axis along the trough. When measured to 10% of maximum amplitude, this axis is close to 400 km. The amplitude of the pressure perturbation is 2 hPa and the temperature anomaly 2 K. The relative vorticity also follows the same shape and has an amplitude of 0.5f at 925 hPa. Here f is the Coriolis parameter. We mentioned that the disturbance is initiated by the "the vacuum cleaner effect" caused the approaching upper level PV anomaly. Relative to the low-level flow, the upper air disturbance moves towards the east. In this way the largest vertical velocities are found at the eastern side of the PV anomaly. Maximum vertical velocity is found at the top of the PBL along the cross-section marked in Fig. 4d and shown in Fig. 5. The ageostrophic wind shows a vertical circulation tilting towards the PV anomaly. Cyclonic vorticity is created below the maximum updraught and anti-cyclonic vorticity above. The precipitation amounts are so far small and a corresponding integration without latent heat release shows nearly the same result.

The polar low develops to a mature warm core disturbance in the next 18 h. The cyclogenesis seems to follow a normal baroclinic development of a reversed shear flow. However, we will show that release of latent heat plays a substantial role. The disturbance moves towards the southeast with

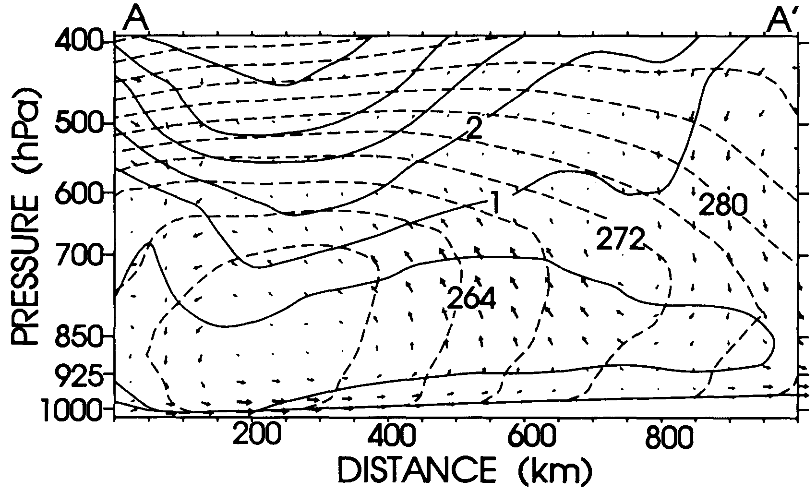

Fig. 5. Cross-section of θ_e (dashed lines, contour step 4 K), PV (solid lines, contour step 1 PVU, 1 PVU = 10^{-6} m^2 s^{-1} K kg^{-1}) and ageostrophic tangential flow (arrows) resulting from a 6 h simulation valid at 18 UTC 13 March 1992 (Case D). The length of an arrow corresponds to a 30-min trajectory. The position of the cross-section is marked with the line AA′ in Fig. 4d.

a speed of 15 m s^{-1}, in the opposite direction of the low-level thermal wind. This gives a steering level at 700 hPa. The SLP and θ_e in the PBL after 24 h simulation are shown in Fig. 6. Also the area of maximum upward vertical velocity is displayed in the figure. The wind relative to the low and the vorticity at 925 hPa are shown in Fig. 7.

After 12 h of integration, the disturbance has kept its shape (not shown), but the amplitudes have increased to 4 hPa in pressure, 4 K in temperature and 1.5f in vorticity. The temperature wave has a normal shape for reversed shear developments: The warm front at the northern side and the cold front at the southern side. Maximum vertical velocities and precipitation are connected to the warm front. The precipitation amounts are now 1 mm per hour.

Twelve hours later (24-h simulation) the cold air has secluded the warm air and the warm anomaly has taken a circular shape, but with a band northwards along what we may call the back-bent warm front (Shapiro and Keyser, 1990) (Fig. 6). In this way the polar low has a typical comma shape. The diameter of the circular part is close to 350 km. The amplitude in SLP is about 8 hPa, the temperature anomaly 6–7 K and the vorticity 4f. Maximum surface wind is 30 m s^{-1}, found at the western side. The wind generated by the disturbance is 15 m s^{-1} (Fig. 7). The largest amounts of precipitation (2 mm an hour) are still found on the western side of the low, along the back-bent warm front and the secluded core.

Later, the polar low continues to move towards the southeast with the same strength for the rest of the simulation (36 h). The largest precipitation amounts are much as before and still found at the western side. The polar low keeps its contact with the back-bent warm front.

The second polar low further north has a distinct anomaly in the surface temperature in the beginning of the simulation with relative vorticity equal to f. Already after six hours of simulation a positive PV anomaly has been formed from the main upper level PV anomaly (Fig. 4c). The development follows a clear baroclinic development with interaction between the upper level PV anomaly and the surface anomaly. After 12 h, the warm front is distinct and the cold air has started to surround the warm air on the southern side. The scale of the low is a little larger than in the first low (diameter 450 km). The seclusion process has now started and 12 h, later a secluded circular warm core is shown (Fig. 6). The vorticity is 3f. Also now the perturbation has a band along the back-bent warm front, but as measured by the vorticity it is weaker than for the first low. Therefore the circular shape is more apparent. The wind relative to the low shows a similar strength as is the first low

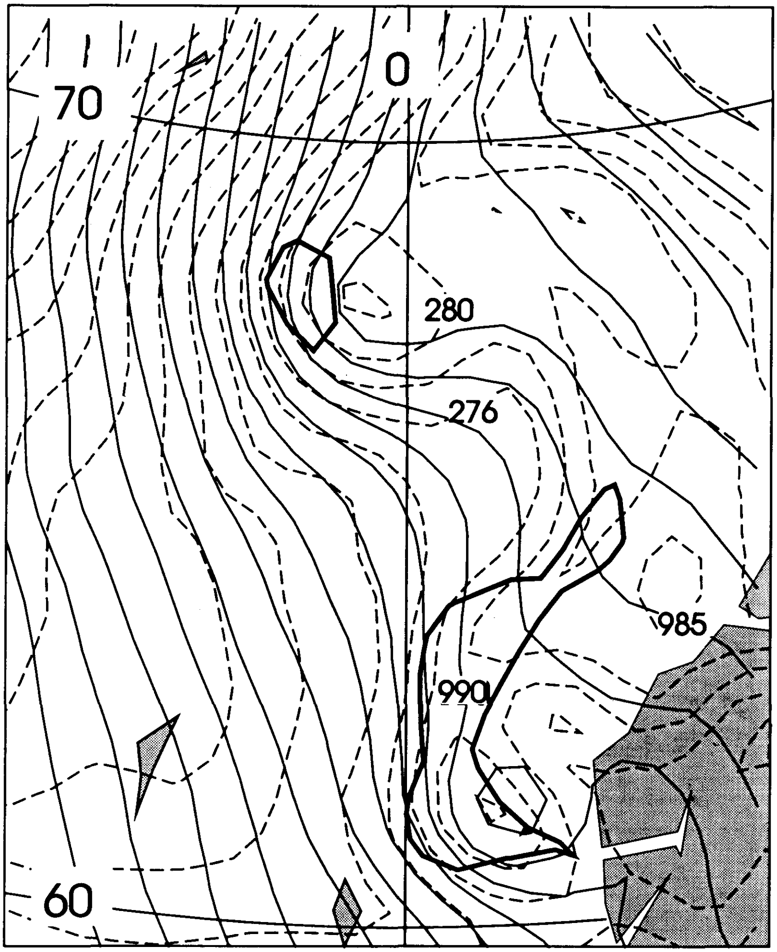

Fig. 6. Simulation (24 h) of SLP (solid lines, contour step 2.5 hPa) and θ_e (dashed lines, contour step 4 K) at the 925 hPa surface. The fields are valid at 12 UTC 14 March 1992 (Case D). The areas encircled with heavy lines have an upward motion, ω, of $\omega \leqslant -1$ Pa s^{-1} at approximately 850 hPa.

(Fig. 7). During the first 12 h, the precipitation amounts, which also here is found at the western side, are similar to those found in the first low. However, later the amounts were about two third of the those in the first low. During the rest of the simulation the low is slowly weakened. It does not keep its circular shape, but is being deformed and stretched horizontally.

The vertical structure of the lows clearly demonstrates the baroclinic nature of the evolution. Fig. 8 shows the 500 hPa height together with the SLP. The disturbances have both a clear tilt towards southeast as expected in a reversed shear flow. Fig. 9a through to d show cross-sections from west to east through both lows after 24 h. Both cross-sections show similar structures. The warm core anomalies have typical patterns in θ_e reaching 550 hPa. Maximum anomalies are found at the surface and a weaker upper maximum at 600 hPa. The θ_e structure is almost vertical, while the vorticity maximum tilts eastwards. On the western side the PBL is shallow with a strong inversion at the top. The eastern side is dominated by the cold air connected to the folding of upper air PV, in agreement with a baroclinic development.

The warm air on the western side is ascending

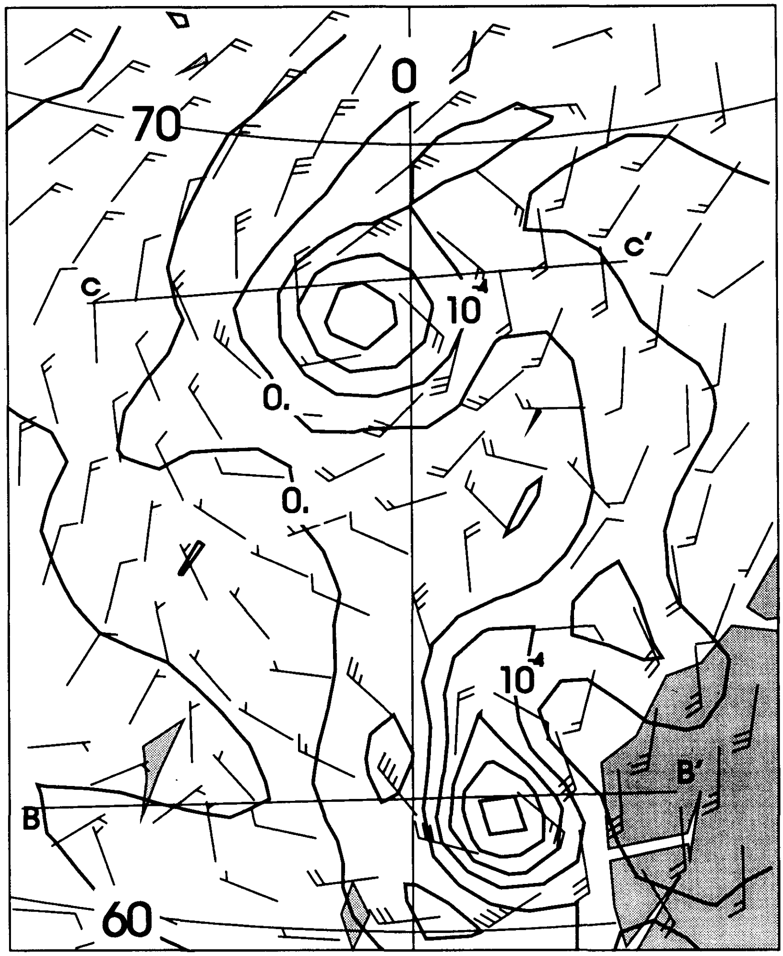

Fig. 7. Simulation (24 h) of relative vorticity (solid lines, contour step 1×10^{-4} s^{-1}) and horizontal wind relative to the moving polar low (arrows) at 925 hPa. A full barb is 5 m s^{-1} and a half barb is 2.5 m s^{-1}. Valid at 12 UTC 14 March 1992 (Case D).

and the cold air at the eastern side is descending, as is normal for a baroclinic development. The ascending air is caused by the surface anomaly as it moves towards the northwest relative to the surface flow. In addition comes the effect of released heat. The ascending air shows maximum vertical velocities between 800 and 700 hPa. In this layer also the maximum amounts of latent heat is released. Relative vorticity is produced below this layer and positive vorticity above. At the surface the vorticity produced is advected toward the low centre and remains in the warm core during the seclusion process. The anti-cyclonic vorticity aloft is being advected outwards. In this way we get a pronounced tilt between the two vorticity anomalies.

Latent heat release strengthens the seclusion process in two ways: In forming a low-level PV anomaly below the heat source mentioned above and in formating a positive PV streamer (Appenzeller and Davies, 1992) from the main upper air PV anomaly. The upper air PV anomaly is diluted above the heat source. This has a large effect in forming the PV streamer seen at the cross-sections in Fig. 9 and horizontally at the 275 K surface in Fig. 10. As expected in a reversed shear case, the

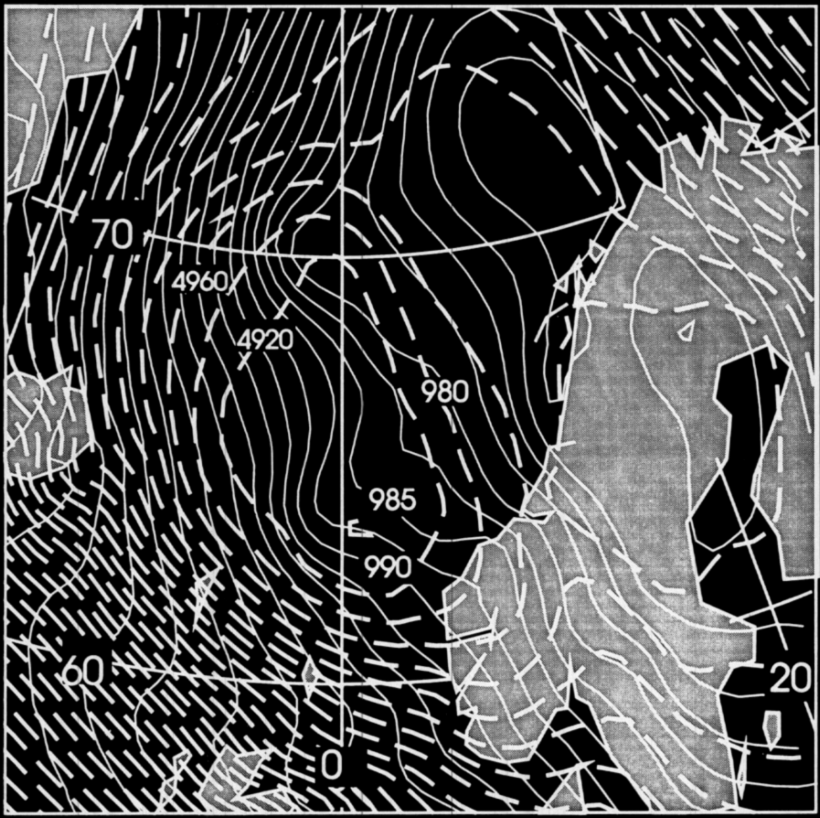

Fig. 8. Simulation (18 h) of SLP (solid lines, contour step 2.5 hPa) and geopotential height (dashed lines, contour step 20 m) at 500 hPa. Valid at 06 UTC 14 March 1992 (Case D).

streamer is formed on the southern side of the low and circles around it. This is made possible by the PV minimum above the heat source. It seems probable that this PV structure contributes to the vertical structure of the polar low in the PBL.

When the model is run without latent heating two weaker polar lows are formed at the same positions with the same translation speed. As expected in a baroclinic development with a reversed shear, the disturbances takes the form of troughs at the surface and no closed isobars are found. The vertical tilt towards southeast is now also found in the PBL. The amplitude of the disturbances in pressure, temperature, vorticity and relative wind is close to 60% of the amplitudes shown with latent heat included. The seclusion process is less developed. In this way the disturbances keep more of its ellipsoid form throughout the simulation. The difference between the two simulations is best characterized by the difference in the seclusion process.

Surface weather maps (not shown) and satellite images also show a polar low being formed in the area east of Iceland and advected towards the coast of southern Norway. The observation seems to verify the scale and the strength of the simulated low. However, the simulated low arrived 3 to 6 h too early at the Norwegian coast. The second polar low is more difficult to verify because of fewer observations. A disturbance is present, but little can be said about its strength. Also for this polar low the simulated timing seems to be rather poor.

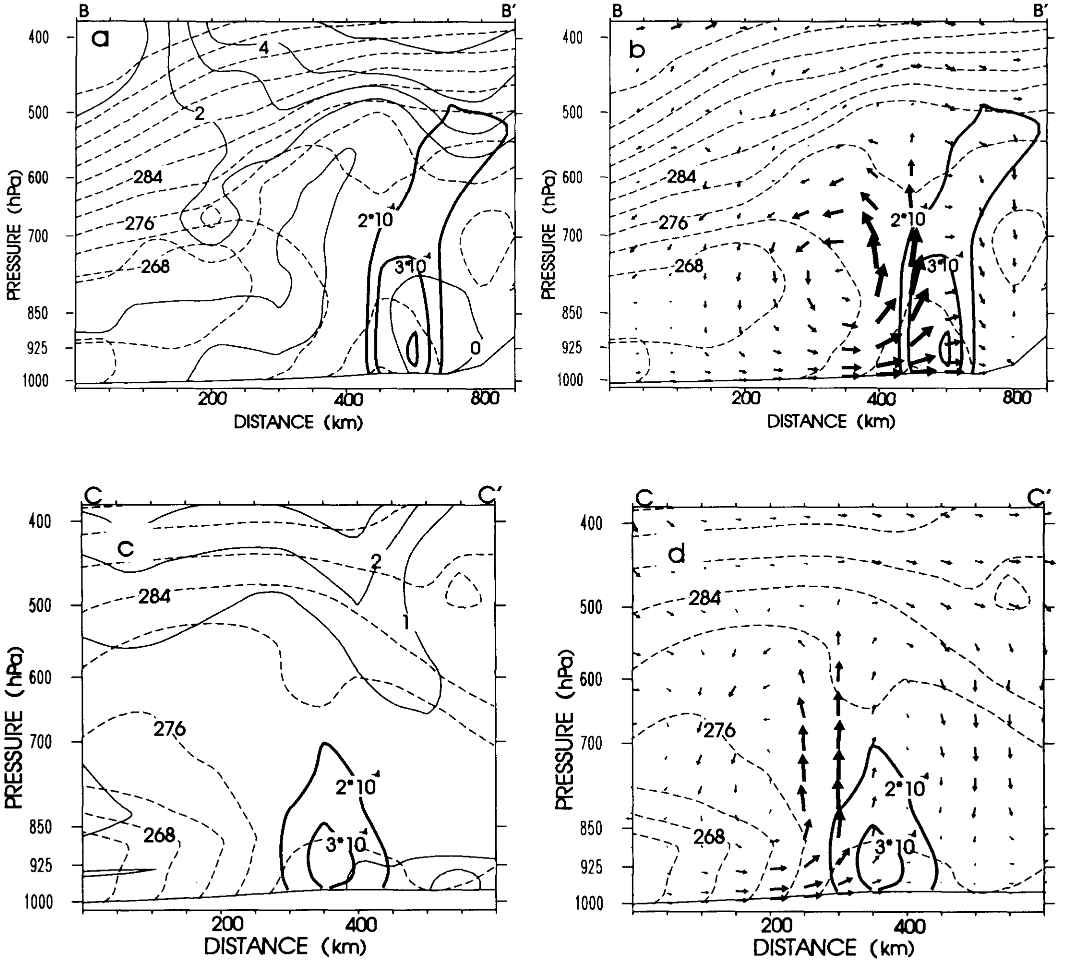

Fig. 9. (a) Cross-section of 24 h simulated of θ_e (dashed lines, contour step 4 K), PV (solid lines, contour step 1 PVU, 1 PVU $= 10^{-6}$ m^2 s^{-1} K kg^{-1}). The area encircled with heavy lines has relative vorticity values greater or equal to 2×10^{-4} s^{-1}. The position of the cross-section is marked with the line BB′ in Fig. 7. The cross-section is valid at 12 UTC 14 March 1992. (b) Same cross-section and time as in (a), but PV is replaced with ageostrophic tangential flow (arrows). The length of an arrow corresponds to a 30-min trajectory. The position of the cross section is marked with the line BB′ in Fig. 7. (c) Same as (a), but for position CC′ in Fig. 7. (d) Same as (b), but for position CC′ in Fig. 7.

6. Concluding remarks

Four apparently similar synoptic situations have been investigated to find the synoptic structures that activate Arctic outbreak polar lows. In two of the cases polar lows developed, and in the other two no polar low was observed. The synoptic situations are characterized by a mature extra-tropical cyclone over Scandinavia. In two ways those lows lead to appropriate synoptic conditions for polar lows to develop. The Arctic outbreak with the Arctic inversion at the top of the convective PBL is being formed as cold air from the ice is advected out over the warm ocean, and the stratospheric, dry intrusion which occurs at the western side of the low. Such an intrusion leaves a marked reservoir of positive PV at low levels, above the baroclinic, convective PBL.

Fig. 10. Simulation (24 h) of PV at the 275 K surface (contour levels: 0.5, 1.5 and 2.5 PVU, 1 PVU = 10^{-6} m^2 s^{-1} K kg^{-1}). Valid at 12 UTC 14 March 1992 (Case D).

Favourable conditions for polar low formation are then present. Baroclinic instability is the obvious mechanism to consider. Beneath the PV anomaly aloft, the vertical stability is low and in this way a local area with deeper convection may be organized. This means that also CISK is a possible instability mechanism.

Our findings suggest a modification of the definition of the *Arctic front polar low* class in the classification of polar lows proposed by Businger and Reed (1989). They found that this type is characterized by shallow baroclinicity and strong surface fluxes. We chose to call this class *Arctic outbreak polar lows* since they do not form at the leading edge of the Arctic front. It seems evident that a mobile upper disturbance is also active. In this respect our findings support earlier statements by for instance Økland (1989), and Nordeng and Rasmussen (1992) that upper air disturbances always seem to be present in the development of polar lows. The presence of an upper disturbance, using the PV concept, should therefore be included in the definition. Based on this modification, necessary conditions for forming Arctic outbreak polar lows are present in all our cases.

Investigation of the corresponding numerical simulations suggests a simple parameter for prediction of the risk of polar low formation. This parameter is given by the height difference between the height of the tropopause, defined as the 2 PVU surface, and the top of the convective PBL underneath. This distance may be regarded as the inverse of a simplified Rossby height, which is a measure of mutual interaction of an upper PV anomaly and a temperature anomaly below in the PBL. In our cases this distance was more than 2500 m in the two cases when no polar lows occurred. For the cases when development took place, the distance was 1000 m or less. There is one exception when this height difference is larger, but in this case the surface anomaly was large before interaction started. Our sample is of course very small and operational experience should be gained before stronger conclusions can be made.

We recommend two horizontal maps for operational forecasting of polar lows. The first shows the height (or θ) of a PV surface representing the tropopause (2 PVU in our examples). Such a map has been proposed many times for weather forecasting, first of all by Hoskins. There is a practical difficulty in constructing such a PV map, since a PV surface might be vertical and even have several crossings along a vertical axis. However, a practical solution may be found. The second map shows the height of the convective boundary layer together with (equivalent) potential temperature in this layer.

Numerical simulations of one situation (Case D) have been more closely examined to get a detailed description of two polar low developments. Relative to the main northerly flow, the developed lows show circular low-level disturbances with diameters of 350 and 400 km, wind 15 m s^{-1} relative to the lows, and maximum relative vorticity 4 and 3f respectively. Baroclinic instability, finite amplitude disturbances in a reversed shear flow, was the main mechanism behind the development. Accordingly, in the beginning troughs were developed at the surface and more circular disturbances aloft. The tilt is in the direction of the displacements of the lows, warm air on the rear side is ascending and cold air in front of the low is descending.

The initial surface temperature waves seclude within 18 h. With the seclusion closed surface isobars are being formed and the polar lows take a vertical circulation structure in the PBL. The surface flow rotates around the secluded warm air, but have a branch of vorticity northward along the back-bent warm front. In this way the lows have a typical comma shape.

Moist processes increase the circulation substantially. Released latent heat was found necessary to seclude the polar lows and to get the vertical structure of the disturbance close to the surface. The heat is released on the western side of the low along the back-bent warm front. PV is then increased below the heat source and diluted above. In the boundary layer PV is difficult to compute and therefore relative vorticity has been displayed instead. The low-level increase of vorticity remains within the warm air in the seclusion process and strengthens the circulation. The upper PV dilution is found to be vital in forming an upper PV streamer from the main PV reservoir. This effect makes the streamer circle cyclonically around the low-level perturbation. The circular shape helps to maintain the vertical low-level structure. No CISK inside the vortex takes place in our simulations.

The two lows (Case D) have a somewhat different initiation. The first is started by the vertical velocities created by the approaching PV anomaly aloft. In this way a small disturbance ensues in the baroclinic flow at the surface. The second low starts from a larger surface anomaly, formed over the warm tongue of ocean surface west of Spitsbergen. The two lows seem to form independently of each other.

This development contains all the ingredients of the conceptual model with "induced self development (ISD)" and diabatic intensification introduced by Montgomery and Farrel (1992). Compared with the ideal simulations carried out by these authors, the scales and the amplitudes are here far smaller. The special circumstance for Arctic polar lows is the deep, convective PBL and the low tropopause, which give ideal conditions for mutual interaction between upper and lower PV anomalies. A large Rossby height might then be obtained even with a small horizontal scale of the disturbance. In westerly flows the Arctic inversion and the strong low-level baroclinicity is normally lacking, and more homogenous regions of deep convection are observed in the cold air masses behind extratropical cyclones. Polar lows of this class are therefore normally not observed under such conditions.

Case C gives a polar low development which is described in Nordeng and Rasmussen (1992). The characteristics of our Case D resembles some of their findings quite well. One main difference is that the Case C polar low appears as a subsynoptic re-intensification of the parent low. Due to the small distance between the parent low and the polar low, the θ_e and relative vorticity fields differ somewhat between the two cases during the initial development. However, when the Case C polar low makes landfall it has become more separated from the parent low, the characteristic seclusion and relative vorticity structure have become quite similar to the development described here. Nordeng and Rasmussen discussed the significance of "the eye" of their cyclone and found tendencies for descending air in the middle of the low. An eye is a sign of CISK taking place. No eye was found in our cases, not even when the resolution in the numerical model was increased substantially.

7. Acknowledgements

We would like to express our appreciation for the valuable assistance bestowed by Mr. F. Cleveland, Mr. A. Foss and Ass. Prof. E. Raustein. We are also indebted to Reviewer B for a well informed and constructive review. This work has also received support from the Norwegian Super Computing Committee (TRU) through a grant of computing time.

REFERENCES

Appenzeller, C. and Davies, H. C. 1992. Strucures of stratospheric intrusions into the troposphere. *Nature* **358**, 570–572.

Blumen, W. 1979. On the short wave baroclinic instability. *J. Atmos. Sci.* **36**, 1925–1933.

Bratseth, A. M. 1985. A note on CISK in polar air masses. *Tellus* **37A**, 403–406.

Browning, K. 1990. Organization of clouds and precipitation in extratropical cyclones. In: Extratropical cyclones. *The Eric Palmen Memorial Volume*, eds.

C. Newton and E. O. Holopainen. Amer. Met. Soc., pp. 129–153.
Businger, S. 1987. The synoptic climatology of polar low outbreaks over the Gulf of Alaska and Bering Sea. *Tellus* **39A**, 307–325.
Carleton, A. M. 1985. Satellite climatological aspects of the "polar low" and "instant occlusion". *Tellus* **37A**, 433–450.
Duncan, C. N. 1977. A numerical investigation on polar lows. *Quart. J. Roy. Meteor. Soc.* **103**, 255–268.
Duncan, C. N. 1978. Baroclinic instability in a reversed shear flow. *Met. Mag.* **107**, 17–23.
Emanuel, K. A. 1986. An air-sea interaction theory for tropical cyclones. Part I: Steady-state maintenance. *J. Atmos. Sci.* **43**, 585–604.
Emanuel, K. A., Fantini, M. and Thorpe, A. J. 1987. Baroclinic instability in an environment of small stability to slantwise moist convection. Part I: Two-dimensional models. *J. Atmos. Sci.* **44**, 1559–1573.
Emanuel, K. A. and Rotunno, R. 1989. Polar lows as Arctic hurricanes. *Tellus* **41A**, 1–17.
Farrell, B. F. 1982. The initial growth of disturbances in a baroclinic flow. *J. Atmos. Sci.* **39**, 1663–1686.
Farrell, B. F. 1984. Modal and non-modal baroclinic waves. *J. Atmos. Sci.* **41**, 668–673.
Farrell, B. F. 1992. The initial growth of disturbances in a baroclinic flow. *J. Atmos. Sci.* **39**, 1663–1668.
Gall, R. J. 1976. The effects of latent heat release in growing baroclinic waves, *J. Atmos. Sci.* **33**, 1686–1701.
Grønås, S. and Hellevik, O. E. 1982. *A limited area prediction model at the Norwegian Meteorological Institute*. Techn. Rep. 61, Det Norske Meteorologiske Institutt, HP.O. Box 43, 0313 Oslo, Norway.
Grønås, S., Foss, A. and Lystad, M. 1987. Numerical simulations of polar lows in the Norwegian Sea. *Tellus* **39A**, 334–354.
Grønås, S. and Midtbø, K. H. 1987. Operational multivariate analyses by successive corrections. In: *Short- and medium-range numerical weather prediction*. Special Volume of the Jap. Met. Soc. Jpn., Tokyo, Japan.
Grønås, S. 1992. Polar Lows. *Proceedings of ECMWF Seminar on Validation of models over Europe*, 7–11 September 1992, Vol. I, pp. 67–90. Available from ECMWF, Shinfield Park, Reading, RG6 9AX, UK.
Harrold, T. W. and Browning, K. A. 1969. The polar low as a baroclinic disturbance. *Quart. J. Roy. Meteor. Soc.* **95**, 710–723.
Hoskins, B. J., McIntyre, M. E. and Robertson, A. W. 1985. On the use and significance of isentropic potential vorticity maps. *Quart. J. Roy. Meteor. Soc.* **111**, 877–946.
Joly, A. and Thorpe, A. J. 1989. Warm and occluded fronts in two-dimensional moist baroclinic instability. *Quart. J. Roy. Meteor. Soc.* **115**, 513–534.
Lystad, M. (Ed.) 1986. *Polar lows in the Norwegian, Greeland and Barents Seas*. Final Rep., Polar Lows Project, The Norwegian Meteorological Institute, Oslo, 196 pp.
Mansfield, D. A. 1974. Polar lows. The development of baroclinic disturbances in cold air outbreaks. *Quart. J. Roy. Meteor. Soc.* **100**, 541–554.
Montgomery, M. T. and Farrell, B. F. 1991. Moist surface frontogenesis associated with interior potential vorticity anomalies in a semigeostrophic model. *J. Atmos. Sci.* **48**, 343–367.
Montgomery, M. T. and Farrell, B. F. 1992. Polar low dynamics. *J. Atmos. Sci.* **49**, 2484–2505.
Nordeng, T. E. 1986. *Parameterization of physical processes in a 3 dimensional numerical weather prediction model*. Tech. Rep. 65, Det Norske Meteorologiske Institutt, P.b. 43, 0313 Oslo.
Nordeng, T. E. and Rasmussen, E. 1992. A most beautiful polar low. A case study of a polar low development in the Bear Island region. *Tellus* **44A**, 88–99.
Økland, H. 1977. *On the intensification of small-scale cyclones formed in very cold air masses heated over the Ocean*. Inst. Rep. Ser. No. 26, Institutt for Geofysikk, Universitetet, Oslo, 25 pp.
Økland, H. 1983. Modelling the height, temperature and relative humidity of a well-mixed planetary boundary layer over a water surface. *Boundary-Layer Meteor.* **25**, 121–141.
Økland, H. 1987. Heating by organized convection as a source of polar low intensification. *Tellus* **39A**, 397–407.
Økland, H. 1989. On the genesis of polar lows. In: *Polar and arctic lows*, eds. P. F. Twitchell, E. Rasmussen and K. L. Davidson. A Deepak Publishing, VI, USA, pp. 179–190.
Ooyama, K. 1982. Conceptual evolution of the theory and modeling of the tropical cyclone. *J. Meteor. Soc. Japan* **60**, 369–380.
Rasmussen, E. 1977. *The polar low as a CISK phenomenon*. Rep. No. 6, Inst. Theoret. Meteor., Københavns Universitet, Copenhagen, 77 pp.
Rasmussen, E. 1979. The polar low as an extratropical CISK disturbance. *Quart. J. Roy. Meteor. Soc.* **105**, 531–549.
Reed, R. J. 1979. Cyclogenesis in polar air streams. *Mon. Wea. Rev.* **107**, 38–52.
Reed, R. J. and Duncan, C. N. 1987. Baroclinic instability as a mechanism for the serial development of polar lows: A case study. *Tellus* **39A**, 376–384.
Shapiro, M. A. and Keyser, D. 1990. Fronts, jet streams and the tropopause. In: Extratropical Cyclones. *The Eric Palmen Memorial Volume*, eds. C. Newton and E. O. Holopainen. Amer. Met. Soc., pp. 167–191.
Staley, D. O. and Gall, R. L. 1977. On the wavelength of maximum baroclinic instability. *J. Atmos. Sci.* **34**, 1679–1688.
Sundqvist, H., Berge, E. and Kristjansson, J. E. 1989. Condensation and cloud parameterization studies with a mesoscale NWP model. *Mon. Wea. Rev.* **117**, 1641–1657.

van Delden, A. 1989a. Gradient wind adjustment, CISK and the growth of polar lows by diabatic heating. In: *Polar and arctic lows*, eds. P. F. Twitchell, E. Rassmussen and K. L. Davidson. A Deepak Publishing, VI, USA, 109–130.

van Delden, A. 1989b. On the deepening and filling of balanced cyclones by diabatic heating. *Meteorology and Atmospheric Physics* **40**.

Wiin-Nielsen, A. 1989. On the precursors of polar lows. In: *Polar and arctic lows*, eds. P. F. Twitchell, E. Rasmussen and K. L. Davidson. A Deepak Publishing, VI, USA, 179–190.

Wilhelmsen, K. 1985. Climatological study of gale-producing polar lows near Norway. *Tellus* **37A**, 451–459.